

Quantifying the risk of power loss in PV modules due to micro cracks

M. Köntges¹, I. Kunze¹, S. Kajari-Schröder¹, X. Breitenmoser² and B. Bjørneklett²

¹Institute for Solar Energy Research Hamelin (ISFH), Am Ohrberg 1, D-31860 Emmerthal, Germany

³REC Solar AS, Kjølboveien 29, NO-1302 Sandvika, Norway

ABSTRACT: Micro cracks in wafer based silicon solar cell modules are nowadays identified by a human observer with the electroluminescence (EL) method. However, the essential question of how the micro cracks affect the PV module performance has yet to be answered. We experimentally analyze the direct impact of micro cracks on the module power and the consequences after artificial aging. We show that the immediate effect of micro cracks on the module power is small, whereas the presence of micro cracks is potentially crucial for the performance of the module after artificial ageing. This confirms the necessity to develop the means of quantifying the risk of power loss in PV modules with cracked solar cells in their lifetime, in order to enable manufacturers to discard defective modules with high risk of failure while keeping modules with uncritical micro cracks. As a first step towards a risk estimation we develop an upper bound for the potential power loss of PV modules due to micro cracks in the solar cells. This is done by simulating the impact of inactive solar cell fragments on the power of a common PV module type and PV array. We show that the largest inactive cell area of a double string protected by a bypass diode is most relevant for the power loss of the PV module. A solar cell with micro cracks, which separate a part of less than 8% of the cell area, results in no power loss in a PV module or a PV module array for all practical cases. In between approximately 12% to 50% of inactive area of a single cell in the PV module the power loss increases nearly linearly from zero to the power of one double string.

Keywords: PV module, micro cracks, lifetime

1. Introduction

Micro cracks in solar cells are a genuine problem for photovoltaic (PV) modules [1-3]. They are hard to avoid and, up to now, basically impossible to quantify in their impact on the efficiency of the module during its lifetime. In particular, the presence of micro cracks may have only a marginal effect on the power of a new module, as long as the different parts of the cell are still electrically connected. However, as the module ages and is subjected to thermal and mechanical stresses, a repeated relative movement of the cracked cell parts can result in a complete electrical separation, thus resulting in inactive cell parts.

Ideally, cells with micro cracks are already identified and rejected before they are integrated into the cell string. This is achieved within the production using e.g. ultrasonic methods [4], thermal flux thermography [5] or electroluminescence (EL) imaging [6]. However, even if this is done perfectly, during string and module production new micro cracks may occur. For a PV module the micro cracks can only be detected using EL imaging. However it is highly undesirable to reject any and every whole string or PV module with some micro cracks, as many of these might still meet the warranted quality over the whole lifetime of the module. It is therefore imperative to develop reliable guidelines to facilitate the decision of string or module rejection due to micro cracks.

For that purpose we choose the following approach: First we introduce micro cracks into crack-free PV modules by a mechanical load test and measure the immediate influence of micro cracks on the module power. We then perform an accelerated aging test on these PV modules to analyze the impact of the micro cracks on the resulting power degradation. Finally we develop an upper bound for the power loss due to micro cracks by simulating the electrical properties of a PV module and a PV module array with the extreme scenario of inactive cell parts.

2. Experimental analysis of the impact of micro cracks on the PV module power

The qualitative consequences of micro cracks in PV modules are commonly known [7]. But in order to

progress in the comprehension of quantitative impact of micro cracks on the module power, it is necessary to perform some systematic experimental studies. In particular, for a good comparability of the results, it is crucial to perform the same test sequence on several modules of the same type.

2.1 Experimental setup

To test the relevance of cell micro cracks to the module power we use sixteen 60-cell PV modules with 15.6 cm x 15.6 cm crack-free multi-crystalline solar cells of the same type. The PV module power is measured by a cetis class AAA HALM flasher with a reproducibility of $\pm 0.1\%$ in module power for repeated measurements at standard test conditions.

An in-house developed mechanical load test equipment complying with the requirements of IEC 61215 10.16 (mechanical load test) is used as a standardized way to insert micro cracks in the solar cells within the PV modules. The test is performed using the high pressure snow load option. The mounting during the mechanical load test was varied for the different modules in order to systematically introduce significantly different numbers of micro cracks into the module cells. To stress the micro cracks caused by the mechanical load test an accelerated aging by a humidity freeze test according to IEC 61215 10.12 with a reduced humid time of 6 h and 200 cycles is performed. Humidity freeze test are carried out on twelve of the sixteen PV modules. The sequential combination of the two tests is effective for cell crack initiation and propagation as well as subsequent electrical interruption of the metallization grid. This testing sequence represents a hostile climate with large temperature fluctuations combined with heavy snow load on the PV module.

For the detection of micro cracks we use an in-house developed EL setup equipped with a "Sensicam qe" camera from PCO using dark field correction. An EL image is taken at the rated short circuit current (I_{sc}) of the PV module and another one at 10% of I_{sc} . To generate the current flow the PV module is forward biased. The image taken at I_{sc} is used for counting the number of cracked cells. The image taken at 10% of I_{sc} is used to identify

inactive cell areas. At this low current the voltage drop across cracks is drastically reduced. So even cell parts with a high crack resistance result in a measurable EL signal, which could not be seen at I_{sc} .

Before and after introducing micro cracks with a mechanical load test and after the humidity freeze test we measure the module power and take EL images. Fig. 1 shows the corresponding flowchart for this test sequence. From the EL images the number of cracked cells is determined. We classify cell micro cracks in the following way, see Fig. 2: cell micro cracks which do not generate inactive cell areas and therewith do not reduce the EL intensity in the I_{sc} picture are classified as mode A cracks. A crack is defined as a mode C crack if an EL image taken at 1/10 of I_{sc} reveals only background noise for the inactive cell part. Cracks seen in one or both of the EL images resulting in cell parts with a reduced intensity but higher than the background noise are defined as mode B cracks.

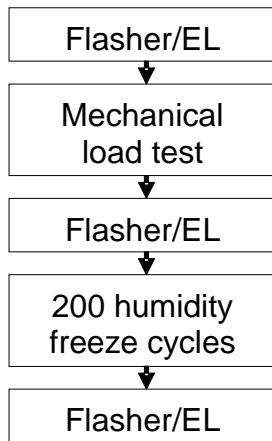


Fig. 1: Schematic of test sequence

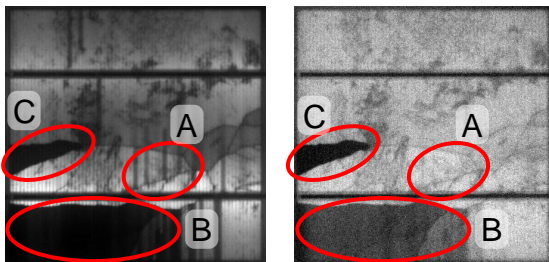


Fig. 2: EL images of the same solar cell with crack modes A, B and C. Left EL image is taken at I_{sc} , right at 10% of I_{sc} .

To evaluate how the power of a PV module decays with time we evaluate the PV module power at several humidity freeze cycles. For this purpose we use an additional PV module of another type with all cells cracked initially in mode A and B.

2.2 Experimental results

The PV module power degradation due to the mechanical load test is shown in dependence of the number of micro cracks introduced by the mechanical load in Fig. 3. Here only PV modules with mode A cell cracks are included in order to assure good comparability of the results. We find that cell micro cracks cause little power loss to a PV module when they do not generate inactive cell areas (mode A). No power loss is detectible if only

some cells crack in mode A. For our 60-cell PV module a power loss of about 1% is measured if half of the cells crack in mode A. From a linear regression of this data a power loss of about 2.5% can be estimated if all cells of the PV module crack in mode A.

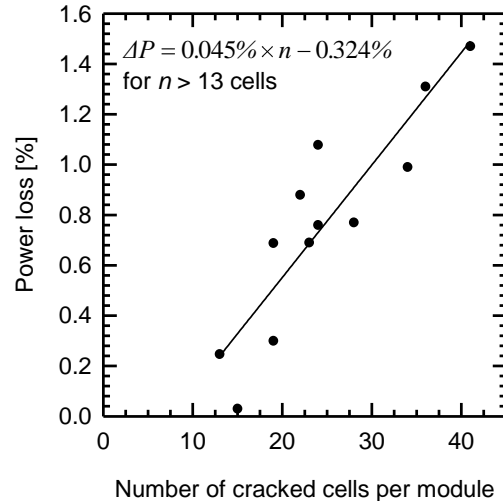


Fig. 3: The power loss for a 60-cell PV module with 15.6 x 15.6 cm² sized cells due to mode A cracked cells is in the range of 0% to 2.5%. The module power is measured before and after introducing the cracks. Each point represents a single PV module.

Fig. 4 shows the power loss after accelerated aging by 200 humidity freeze cycles as function of the number of cracked cells. All modules show strong glass corrosion after the humidity freeze test. This corresponds to a mean degradation of approximately 3% of I_{sc} of all PV modules.

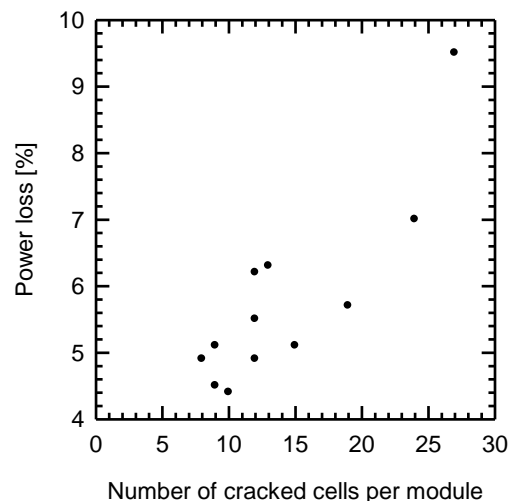


Fig. 4: The power loss after a test sequence of mechanical load and 200 humidity freeze cycles correlates with the number of cells cracked in the mechanical load test. Each point represents a single PV module.

Besides this “degradation offset” we see that the power loss is clearly higher for modules with a higher number of cracked cells after the mechanical load test. The highest power loss found in this test is less than 10%. The electroluminescence images of the degraded PV modules

show that some of the cell cracks changed from mode A to mode B, see Fig. 5. In a few cases the crack mode changed from A to C, see also Fig. 5. These results highlight the importance of micro cracks for the PV module aging. They stress the necessity of understanding the potential power losses due to micro cracks.

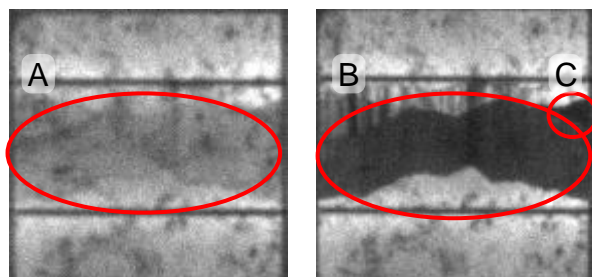


Fig. 5: Example for an EL image of one cell after the mechanical load test showing almost crack mode A micro cracks (left). The right image shows the same cell after 200 cycle humidity freeze (right). Some of the micro cracks changed to crack mode B and one small fraction changes to mode C.

Fig. 6 shows the power loss of a PV module with all cells cracked initially as function of the number of humidity freeze cycles. After an initial drop the power loss rise almost linear as a function of the number of humidity freeze cycles. In contrast to the prior tested PV modules this PV module does not show glass corrosion after 200 humidity freeze cycles. The electroluminescence images taken after each power measurement show crack mode change from A over B to C and even from C back to B, see insets of Fig. 6. But with increasing number of humidity freeze cycles more cracks change from mode A to B and some to mode C. Over all this PV module lose about 10% of power after 200 humidity freeze cycles due to micro cracks.

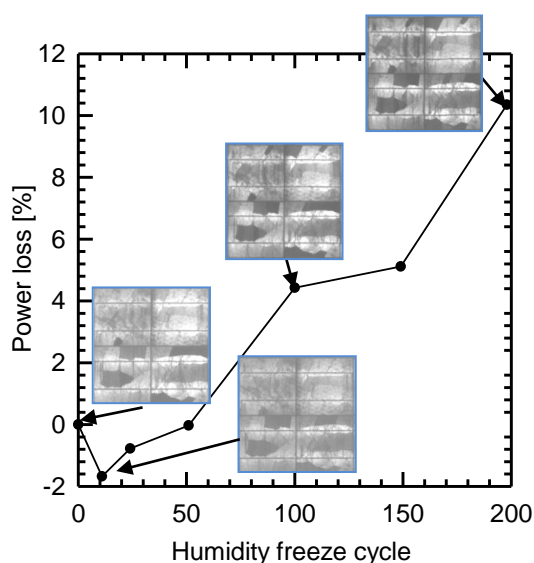


Fig. 6: Power loss of a PV module as a function of number of humidity freeze cycles. The insets show EL images of a PV module section at various number of humidity freeze cycle.

2.3 Discussion

The results of the experimental test sequence of Fig. 1 demonstrate the relevance of micro cracks for the PV module aging and stress the necessity of understanding the potential power losses due to micro cracks. They also show the real challenge in interpreting the relevance of micro cracks for PV module power stability: as we have shown above, mode A cracks in the silicon wafer before artificial ageing only have a small impact on the PV module power, even though the power loss correlates with the number of mode A cracked cells in the module. Nevertheless, when artificial ageing is applied to PV modules with mode A cracked solar cells, the number of micro cracked cells in a module is highly relevant for the power degradation of the PV module. However, the data shown in Fig. 4 are substantially scattered, making a reliable quantitative prediction of the power degradation from the initial EL image quite challenging to say the least. As shown above, some mode A cracks change during artificial ageing to mode B or even mode C cracks. Obviously, in such a case the impact of this crack on the module power will rise. However, up to now it is unknown how and when these changes occur, and with which probability this is to be expected in a given environment. But for a single PV module with all cells cracked we find a linear function of humidity freeze cycle number and therewith in time. This time dependence of power degradation is often measured for PV modules if no visible reason for degradation is found [8]. Micro cracks might be the reason for slow continuous power loss of PV modules in the field without a visible failure.

The question arises, what influences the power loss due to micro cracks. Several aspects are well known, such as the cell thickness, the defect density, the texturing process, the busbar solder technology [9] and quality [2], ribbon yield strength and geometry: all these may influence the rate of wafer fracturing and crack propagation in the silicon wafer [10]. However, for the electrical functionality of the solar cell the crack propagation through the metallization scheme is the primary parameter. Crack propagation into the metal will depend mostly on the thickness and uniformity of the $Al_{12.6}Si_{87.4}$ eutectic of the rear metallization and the ductility and geometry of the silver front metallization.

3. Simulation of power losses due to inactive cell areas

As a first step towards a fundamental understanding of the connection between micro cracks of different modes and the potential power degradation of the PV module, we numerically analyze the impact of mode C cracks, corresponding to inactive cell areas, on the module power. This represents a worst case scenario, in which any area surrounded by micro cracks is immediately electrically isolated from the active part of the cell. As we have seen in the previous section, this is not a regular occurrence and is solely used to develop an upper bound of the potential power degradation and to analyze the influence of different parameters.

3.1 Simulation model

In order to assess how the area of inactive cell components A_{inactiv} influences the PV module output, we carry out an I-V characteristic simulation of a 60-cell PV module with the free software LTSpice from Linear

TechnologyTM. The model parameters used for our simulation are listed and explained in Tab. 1. The electrical PV module parameters are typical for today's multi-crystalline quality PV modules. Fig. 7 shows the circuit diagram of one solar cell.

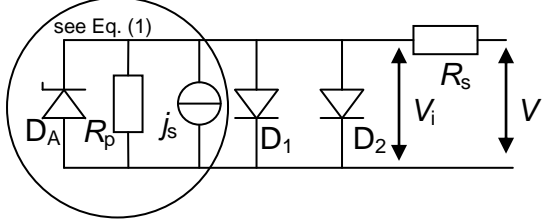


Fig. 7: Equivalent circuit diagram of one solar cell. An avalanche diode is included to simulate the reverse current behavior of the solar cell.

The reverse current I_R composed of the current generation, the current through the parallel resistance and the avalanche breakdown current are modeled by a compact formula published by Alonso-Garcia et al. [11],

$$I_R = \frac{\left(j_{sc} - \frac{V_i}{R_p} \right) \cdot A_{active}}{1 - \exp \left\{ B_c \left(\phi_T - \sqrt{\phi_T^2 - V_b} \right) \left(\phi_T - V_i \right) \right\}} \quad (1)$$

where ϕ_T is an internal barrier, V_b the break down voltage, B_c a material parameter, j_{sc} the short current density at standard test conditions and the parallel resistance R_p of a solar cell. A_{active} is the active area of the solar cell and V_i the internal voltage of the solar cell.

The direct recombination current I_{D1} is modeled by diode D_1 with a standard diode model,

$$I_{D1} = j_{01} \cdot A_{active} \cdot \left(\exp \left\{ \frac{V_i}{V_T} \right\} - 1 \right), \quad (2)$$

where V_T is the thermal voltage at the cell junction.

The Shockly-Read-Hall recombination current I_{D2} is modeled by diode D_2 with an ideality factor of two,

$$I_{D2} = j_{02} \cdot A_{active} \cdot \left(\exp \left\{ \frac{V_i}{2V_T} \right\} - 1 \right). \quad (3)$$

The voltage drop across the series resistance R_s reduces the external cell voltage V to the internal voltage V_i as

$$V_i = V - R_s \cdot (-I_R + I_{D1} + I_{D2}) / A_{active}. \quad (4)$$

The series resistance R_s is a lumped parameter describing the series resistance on the cell, the resistance of the interconnectors and the contact resistance between interconnector and cells.

For the electrical simulation of a cell with a fractured cell part we connected the inactive cell area $A_{inactive}$ in series with a break resistance R_b . These two elements are in parallel to the remaining active cell area A_{active} of that cell, see Fig. 8. The sum of $A_{inactive} + A_{active}$ is 243.35 cm^2 (A_{total}) for each solar cell. To simulate a completely inactive cell area is disconnected from the active cell part. For simplification we introduce a graphical symbol for a broken cell, see Fig. 8b).

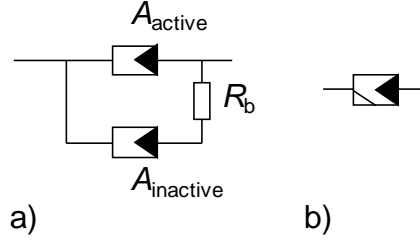


Fig. 8: a) Circuit diagram of a solar cell with a break resistance R_b between cell and the broken cell fraction. b) Graphical symbol for a broken cell.

Table 1: Parameters of the PV module simulation

PV module type	Series connection with three bypass diodes
Number of cells in the module/ number of cells per bypass diode	60/20
Solar cell area A_{total}	243.36 cm ²
Module parameters P_{mpp} ; I_{sc} ; U_{oc} ; I_{mpp} ; U_{mpp}	228 W _p ; 8.36 A; 38.1 V; 7.67 A; 29.7 V
Module temperature	25°C
Light intensity	1000 W/m ²
Inactive cell area of the defective cell	variable
Parameter of IV characteristics in forward voltage for all solar cells	Two diode model
Saturation current J_{01} of first diode with ideality factor one	$5 \times 10^{-13} \text{ A/cm}^2$
Saturation current J_{02} of second diode with ideality factor two	$5 \times 10^{-8} \text{ A/cm}^2$
Series resistance R_s	1.7 Ohm cm ²
Parallel resistance R_p	$1 \times 10^5 \text{ Ohm cm}^2$
Short-circuit current-density j_{sc}	34.35 mA/cm ²
Parameter of IV characteristic in reverse bias for all solar cells	Model of Alonso-Garcia and Ruiz [11]
Dimensionless parameter B_c	3
Built in junction voltage ϕ_T	0.85 V
Breakdown voltage V_b (unless otherwise noted)	15 V

With this model we simulate four scenarios. In scenario I we calculate the power loss of one PV module caused by a single defective cell with a variable inactive area size. Fig. 9 shows the circuit diagram of the whole PV module with one broken cell. The PV module consists of 60 cells in series and 3 bypass diodes each in parallel to 20 solar cells. Below we name these 20 series connected cells plus the parallel by pass diode a double string. In this scenario the inactive area $A_{inactive}$ of that single solar is disconnected. This scenario represents the power loss introduced by a change of the cell crack from mode A to C. We also varied the break down voltage of that defective cell to show the importance of that parameter.

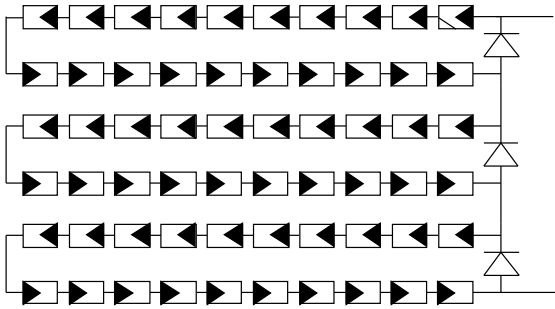


Fig. 9: Circuit diagram used for scenario I & II of one solar module of 60 solar cells and with three by pass diodes. One solar cell is broken in the first double string.

In scenario II we contact the “inactive” cell area by the series break resistance R_b to the active cell part, as shown in Fig. 8. This shows the influence of cell cracks changing from mode A to B in a PV module.

Under realistic conditions often more than one cell of a PV module shows micro cracks. Therefore we simulate in scenario III a module having a varying number of defective cells in a double string. The circuit diagram for scenario III is shown in Fig. 10. On the one hand we simulate 19 cells having the same inactive cell area and one cell with a deviant inactive cell area compared to the others. On the other hand we define a number of cells having an equal size of inactive cell area in a single double string and all other cells of the module are intact.

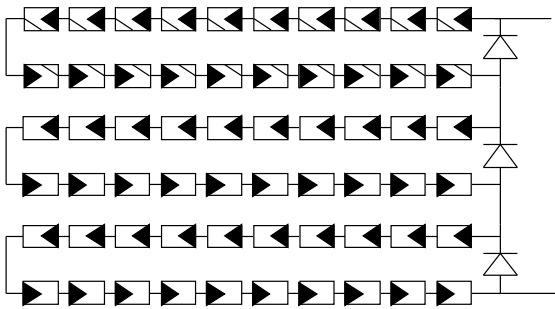


Fig. 10: Circuit diagram used for scenario III. In one double string a various number of cells are broken.

In scenario IV we calculate the power loss of a PV module with a single defective cell in series connected with 19 intact PV modules, see Fig 11. Due to isolation voltage restrictions of today’s modules one would not connect much more than 20 of these PV modules in series to an array. Therefore this scenario shows the upper bound for the power loss due to a single defective cell in a PV module array.

3.2. Simulation results

Scenario I, Influence of inactive cell area and breakdown voltage: The voltage over a defective cell is in forward bias as long as the solar cell in the PV module can carry the module current I_{MPP} . The I_{sc} is the maximum generation current a cell can carry in forward bias and is proportional to the total cell area A_{total} . If the total cell area is reduced so that the I_{sc} of the cell gets below I_{MPP} of the other cells the voltage over the defective cell becomes reverse biased.

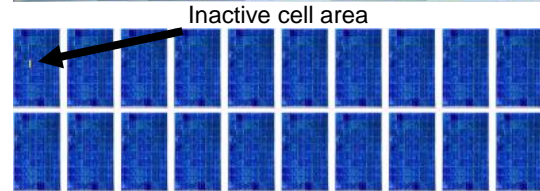
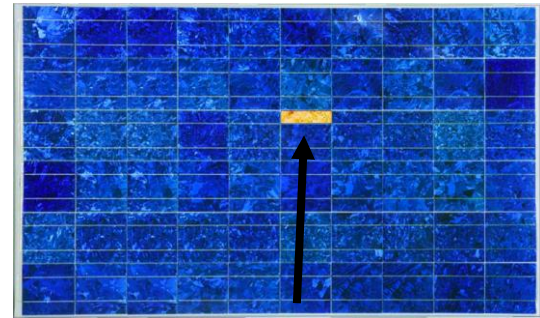


Fig. 11: Schematic for scenario III: PV module array of 20 series connected PV modules. Only a single solar cell in a single the PV module suffers from an inactive cell area.

A defective cell with the inactive cell area $A_{inactive}$ is in forward bias if the following inequation is true:

$$\frac{A_{inactive}}{A_{total}} < \frac{I_{sc} - I_{MPP}}{I_{sc}} \quad (5)$$

Therefore inequation (5) gives a rough estimation to evaluate the power loss due to a defective cell in the module. The right term of inequation (5) is 8.25 % for the parameters used for the simulation shown in Tab. 1. So 8.25% of one single cell in the PV module may be inactive without a significant module power loss.

However, with the simulation we get a more detailed picture of the power loss of a PV module. Fig. 12 shows the simulation of power loss as well as the current in the maximum power point (MPP). These parameters are shown as a function of the size of the inactive area of a single solar cell in the PV module for various breakdown voltages of the solar cell. Clearly the breakdown voltage has a significant impact on the power loss. If the inactive cell area of the defective solar cell in the PV module violates inequation (5), this cell is polarized in reverse bias by the other cells until the current can flow through the defective cell. For the simulation shown here, the inactive cell area $A_{inactiv}$ may cover up to 8% of total wafer area without leading to any relevant power loss, which agrees well with equation (5). For a large 15.6 x 15.6 cm² solar cell 8% equals approximately 20 cm² cell area.

For typical breakdown voltages of more than 15 V, the bypass diode bridges the string with a defective solar cell with an inactive cell area of at least 50%. For this type of solar cell the power loss in dependence of the inactive area is predictable without knowing the exact breakdown voltage. In this case no relevant reverse current flow is possible. This leads to the complete loss of the power of the double string with the defective cell. Before the bypass diode is active, the current flows in the reverse direction over very local areas of the defective solar cell. The current flow under MPP conditions of the module is shown in Fig. 12. For breakdown voltages of 15 V and less the current flows through the reverse biased defective cell and not through the bypass diode.

Especially for solar cells with a breakdown voltage of less than 15 V there is an increasing risk of high local current and power densities with decreasing breakdown voltage. This may lead to hot spots and thus may lead to a local damage of the lamination material [12]. Furthermore with increasing inactive area the current I_{MPP} of the defective module decreases below the nominal I_{MPP} value of the PV module. This low I_{MPP} current is a problem for series connected PV module in a array and is described in scenario IV.

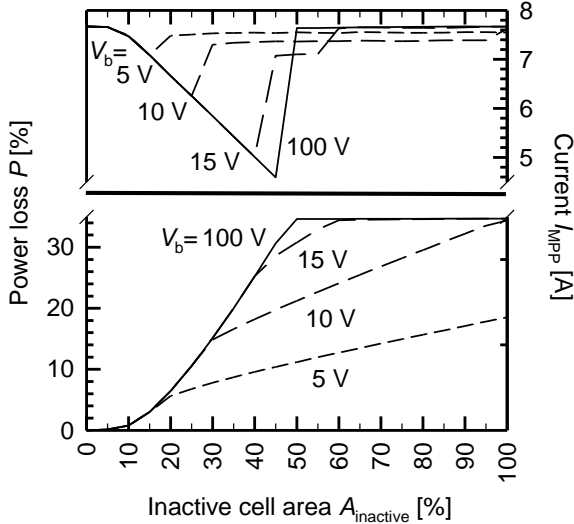


Fig. 12: Simulation of the module power loss (lower part of graph) and the current in the MPP (upper part of graph) for a 60 cell PV module for various breakdown voltages V_b . For one of the sixty $15,6 \times 15,6$ cm² large solar cells the inactive cell area varies from 0% (0 cm²) to 100% (243.36 cm²).

Scenario II, Influence of mode B cracked cells:

Very often cell fragments luminesce less brightly in EL images, but are not yet dark (mode B cracks). In this case the cracked cell area is still electrically connected via a fracture series resistance to the remaining cell. In our simulation we connected this cell area by a series resistance R_b in parallel to the active cell area. Fig. 13 shows the PV module output as a function inactive area and parameterized by the fracture resistance R_b . For 100 % inactive cell area the simulation is equivalent to a PV module with an additional series resistance. In this case the module power is affected if the series resistance is in the magnitude of the source resistance of the intact PV module. For our example the source resistance in the MPP of the intact PV module is 3.9 Ohm. The simulation shows a strong influence on the module power if the fracture resistance R_b is about one Ohm. A fracture resistance of approximately 10 Ohm generates nearly the same power loss as a completely inactive cell part (crack mode C). We stress that the I_{MPP} of that module is only slightly affected as long as the fracture resistance is one order of magnitude lower than the source resistance of the module. This is important for the series connection to a module array described in scenario IV.

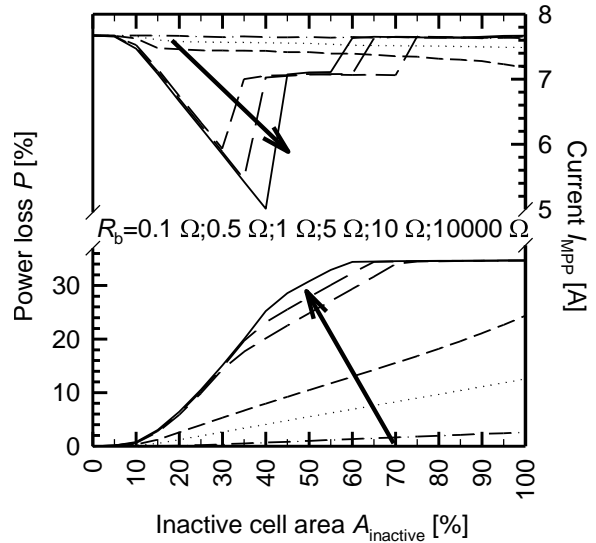


Fig. 13: Simulation of the module power loss (lower graph) and the current in maximal power point (upper graph) with the parameters of Tab. 1. The “inactive” solar cell area is electrically parallel connected to the active cell part by various series break resistances. The series resistance increases in direction of arrow.

Scenario III, Influence of additional defective cells:

We simulate the power loss of a PV module with 20 defective solar cells in a double string. Fig. 14 shows the power loss of the module as a function of the inactive cell area of 19 equal solar cells.

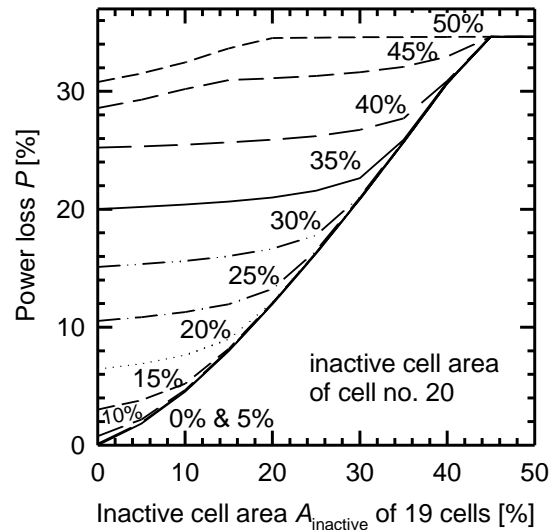


Fig. 14: Simulation of the power loss of a PV module with all cells defective in one double string. All cells have the same inactive cell area except for cell 20. The inactive cell area of cell 20 is shown as parameter. While the inactive cell area of cell 20 exceeds the inactive cell area of the 19 other cells the power loss is dominated by cell number 20.

The inactive cell area of cell number 20 is used as parameter. The simulation shows that a single solar cell (cell no. 20) predominantly determines the power loss of the PV module if it has a 5% larger inactive cell area compared to all the other defective cells. Therefore in

most practical cases the power loss is determined by the cell with the largest inactive cell area per double string. In Fig. 15 the dependence of the module power on the number of cells with equal inactive cell parts in a double string shown. Even in this unlikely case the largest contribution to the power loss is already determined by the presence of one single defective cell.

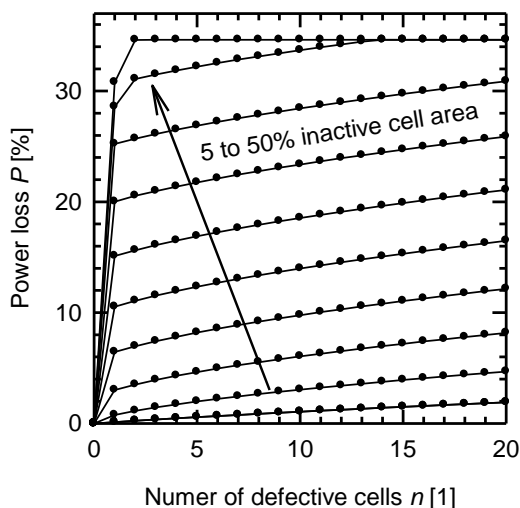


Fig. 15: Simulation of the power loss of a PV module with multiple defective cells in one double string with defective cells having the same inactive cell area.

Scenario IV, Influence on PV module arrays: Due to isolation voltage restrictions of today's modules one would not connect much more than 20 of these PV modules to an array. Therefore Fig. 16 shows the power loss of a single module depending on the inactive cell area of a single solar cell in comparison to the power loss of the same module integrated in series with 19 intact modules. If the current at the MPP of a single PV module is reduced significantly due to defective cells, the power loss of the single PV module does not equal the power loss in a PV module array. In a PV module array, a reduction in the current operating point would lead to a power reduction of all PV modules of the array. This is more disadvantageous in most cases then to operate the defective string at a higher current and thereby waive the power of the broken string at least partly. This effect is comprehensible by the simulated I_{MPP} current in Fig. 16. In extreme cases, the bypass diode bridges the string with the defective cell. For this example Fig. 16 shows that the defective string part loses its power more drastically with increasing inactive area in a PV module array than a single module. For the PV module array again an inactive cell area of 8% is acceptable, see Fig. 16. While a higher inactive cell area is more critical for the power loss of a PV module array compared to a single PV module.

3.3 Discussion

The numerical simulation of the electric properties of PV modules with one or more cells with reduced active area, corresponding to the worst case scenario of mode C cracks, gives valuable insight into the influence of different parameters on the resulting power loss of the PV module considered. We showed that within one PV module the cell with the largest inactive area determines the power loss of

this module. Additionally, even if several cells with exactly the same inactive area occur in one module, which is highly unlikely in realistic circumstances, the cell having the greatest inactive cell area has the highest impact on the module power. This is a highly relevant observation for judging the potential risk of power loss for a given PV module: although the EL image of a module with long micro cracks in most cells but small possible inactive areas may look disastrous, another module with only one defective cell that potentially loses a large fraction of its active area has a higher potential power loss.

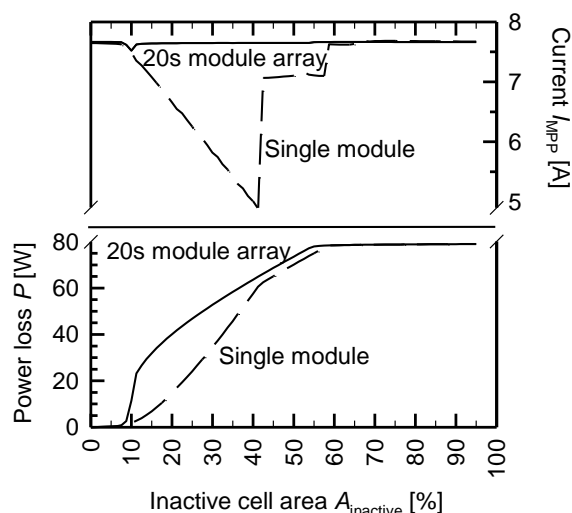


Fig. 16: Simulation of the power loss of a single PV module with a single solar cell having a varying inactive cell area. The simulated power loss of a 20s PV module array containing this defective module is also shown. More than 8% of inactive cell area in the 20s module array leads to a much higher power loss compared to the stand alone PV module.

Another aspect is equally crucial for the evaluation of EL images: as we have shown and explained above, a PV module can tolerate the loss of a certain percentage of the active area of a solar cell without much impact on the module power at all. In the PV module simulated here it lay at about 8% of the total cell area. Again, with this knowledge, adapted for the module type in question, the evaluation of EL images and the subsequent decision of rejection or acceptance of the module stand on a much firmer ground. For a module array the discussed arguments as a basis for decision hold as well. However note that the impact of a defective cell with inactive area above the threshold is much more decisive.

In reality, even under the harsh conditions of artificial ageing, the worst case scenario that all micro cracks revert to mode C cracks is exceedingly unlikely. In the experiments discussed in section 2 only in a few cases a mode A crack reverted to a mode C crack, and not in a single module this occurred for all micro cracks in the module. In contrast we found the cracked areas to be electrically connected to the active cell area to some degree. In the simulations we considered this by connecting the cracked areas with a series resistance to the active cell part. As long as this break resistance is one order of magnitude less than the module resistance in MPP conditions the power loss is low. This may be the reason

why we did not find a more drastically power loss after 200 Humidity freeze cycles in our experiment.

4. Conclusion

We showed that artificially initiated micro cracks in the silicon wafer do not reduce the power generation of a PV module by more than 2.5% relative if the crack does not harm the electrical contact between the cell fragments. However by a subsequent accelerated aging test the crack resistance between cracked cell fractions increase. Furthermore the number of cracked cells correlates with the power degradation after the accelerated aging test and the power loss shows almost a linear dependence of time.

However we do not know the propagation rate for cracks in the wafer to the cell metallization under realistic conditions. This rate depends strongly on the preparation conditions of the solar cells and the PV module. To avoid power loss due to micro cracks two strategies may be possible. The first strategy is to avoid cell breakage. The second strategy may be to use a more flexible cell metallization that prevent electrical isolation of cell parts if the silicon is broken.

For a classification of cracks in the wafer which does not harm the metallization of the cells in the initial state we introduced a computer simulation. We assumed a worst case scenario for the calculation of the power loss due to micro cracks by implying that the cracks isolate cell areas.

We developed some reference points to assess the impact of cell micro cracks to the power of a standard PV module with 60 solar cells. Here we found the power loss due to inactive cell area depends on the breakdown voltage of the solar cells. Only for solar cells with a breakdown voltage of equal or more than 15 V the power loss is calculable in dependence of the inactive cell area without knowing the exact breakdown characteristic of the cell. However for all cases cell micro cracks of less 8% cell area do not influence the module power. In between approximately 12% to 50% of inactive cell area of a single cell in the PV module the power loss increases nearly linear from zero to the power of one double string for cells with a breakdown voltage of equal or more than 15 V. In a string protected by a bypass diode the cell with the largest inactive cell area is most important for the power loss of the PV module. These reference points help to classify PV modules with partly cracked cells.

5. Acknowledgements

Funding was provided by the State of Lower Saxony.

6. References

- [1] S. Pingel, Y. Zemen, O. Frank, T. Geipel and J. Berghold, Mechanical stability of solar cells within solar panels, Proc. of 24th EUPVSEC (WIP, Dresden, Germany, 2009) 3459-3464
- [2] A. M. Gabor, M. M. Ralli, L. Alegria, C. Brodonaro, J. Woods, L. Felton, Soldering induced damage to thin Si solar cells and detection of cracked cells in modules, Proc. of 21st EUPVSEC (WIP, Dresden, Germany, 2006) 2042-2047
- [3] M. Köntges, K. Bothe., Elektrolumineszenzmessung an Photovoltaik-Modulen. *Photovoltaik Aktuell supplement in Elektro Praktiker* 7/8 2008, p. 36-40

- [4] W. Dallas, O. Polupan, and S. Ostapenko, Resonance ultrasonic vibrations for crack detection in photovoltaic silicon wafers, *Meas. Sci. Technol.* **18** (2007) 852–858
- [5] Simina Fluga und Hartmut Eigenbrod, Inline-Thermografie-System prüft Solarzellen – Den Mikrorissen auf der Spur, *QZ* **54** (2009) 9
- [6] T. Fuyuky, H. Kondo, T. Yamazaki, Y. Takahaschi, Y. Uraoka, Photographic surveying of minority carrier diffusion length in polycrystalline silicon solar cells by electroluminescence, *Applied Physics Letters* **86** (2005) 262108.
- [7] P. Grunow, P. Clemens, V. Hoffmann, B. Litzemberger, L. Podlowski, Influence of micro cracks in multi-crystalline silicon solar cells on the reliability of PV modules, Proc. of 20th EUPVSEC (WIP, Barcelona, Spain, 2005) 2042-2047
- [8] C.R. Osterwald, J. Adelstein, J.A. del Cueto, B. Kroposki, D. Trudell, and T. Moriarty, Comparison of degradation rates of individual modules held at maximum power, Proc. of 4th World Conference on PV Energy Conversion (IEEE, Waikoloa, Hawaii, 2006) 2085–2088
- [9] B. Lalaguna, P. Sánchez-Friera, H. Mäckel, D. Sánchez, J. Alonso, Evaluation of Stress on Cells During Different Interconnection Processes, Proc. of 23rd EUPVSEC (WIP, Valencia, Spain, 2008) 2705-2708
- [10] J. Wendt, M. Träger, M. Mette, A. Pfennig, B. Jäckel, The Link Between Mechanical Stress Induced by Soldering and Micro Damages in Silicon Solar Cells, Proc. of 24th EUPVSEC (WIP, Hamburg, Germany, 2009) 3420-3423
- [11] M.C. Alonso-Garcia, J.M. Ruiz, Analysis and modelling the reverse characteristic of photovoltaic cells, *Solar Energy Materials & Solar Cells* **90** (2006) 1105–1120
- [12] W. Herrmann, W. Wiesner, W. Vaaßen, Hot Spot Investigations on PV Modules – New concepts for a tests standard and consequences for module design with respect to bypass diodes, Proc. of 26th PVSC (IEEE, Anaheim, Canada 1997) 1129